

THE DECAYING LONG-PERIOD OSCILLATION OF A STELLAR MEGAFLARE

S. ANFINOGENTOV¹, V. M. NAKARIAKOV^{2,3,4}, M. MATHIOUDAKIS⁵, T. VAN DOORSELAEERE^{6,8}, AND A. F. KOWALSKI^{7,9}

¹ Institute of Solar Terrestrial Physics, Irkutsk, Russia; anfinogentov@iszf.irk.ru

² Centre for Fusion, Space and Astrophysics, Physics Department, University of Warwick, Coventry CV4 7AL, UK

³ School of Space Research, Kyung Hee University, Yongin, 446-701 Gyeonggi, Korea

⁴ Central Astronomical Observatory at Pulkovo of RAS, 196140 St Petersburg, Russia

⁵ Astrophysics Research Centre, School of Mathematics and Physics, Queen's University, Belfast BT7 1NN, UK

⁶ Centre for Mathematical Plasma Astrophysics, Department of Mathematics, KU Leuven, Celestijnenlaan 200B bus 2400, B-3001 Leuven, Belgium

⁷ NASA Goddard Space Flight Center, Code 671, Greenbelt, MD 20771, USA

Received 2013 May 6; accepted 2013 June 27; published 2013 August 5

ABSTRACT

We analyze and interpret the oscillatory signal in the decay phase of the *U*-band light curve of a stellar megaflare observed on 2009 January 16 on the dM4.5e star YZ CMi. The oscillation is well approximated by an exponentially decaying harmonic function. The period of the oscillation is found to be 32 minutes, the decay time about 46 minutes, and the relative amplitude 15%. As this observational signature is typical of the longitudinal oscillations observed in solar flares at extreme ultraviolet and radio wavelengths, associated with standing slow magnetoacoustic waves, we suggest that this megaflare may be of a similar nature. In this scenario, macroscopic variations of the plasma parameters in the oscillations modulate the ejection of non-thermal electrons. The phase speed of the longitudinal (slow magnetoacoustic) waves in the flaring loop or arcade, the tube speed, of about 230 km s⁻¹ would require a loop length of about 200 Mm. Other mechanisms, such as standing kink oscillations, are also considered.

Key words: stars: flare – stars: low-mass – stars: oscillations – Sun: oscillations

1. INTRODUCTION

One of the major recent breakthroughs in solar and stellar atmospheric physics is the discovery of magnetohydrodynamic (MHD) wave activity in the solar corona (e.g., De Moortel & Nakariakov 2012). Waves with periods of several minutes are confidently resolved in time and space with the current array of solar instrumentation and techniques. The propagation characteristics of these waves are known to be strongly affected by structuring, or inhomogeneity, of the coronal plasma by the magnetic field. MHD wave theory (e.g., Zaitsev & Stepanov 1975; Roberts et al. 1984; De Moortel & Nakariakov 2012) distinguishes between the kink, sausage, torsional and longitudinal wave modes. These wave modes have very different physical properties and observational signatures. In particular, for the typically low- β plasma of coronal active regions, the propagation speed of the kink, sausage, and torsional modes is in the range of the Alfvén speed inside and outside the plasma waveguide, while the longitudinal mode propagates at about the sound speed. Sausage and longitudinal modes are essentially compressive. In the sausage mode, the plasma flows are mainly transverse in contrast with the longitudinal mode that is characterized by field-aligned flows. Both sausage and longitudinal modes do not perturb the axis of the waveguiding plasma non-uniformity. The kink mode is compressive too, while it becomes weakly compressive in the long-wavelength regime. The kink mode perturbs the axis of the waveguide. The torsional mode is essentially incompressible and does not perturb the waveguide axis and its boundary. The main interest in coronal waves is connected with their great potential for plasma diagnostics by the method of MHD seismology (e.g., Stepanov et al. 2012). The key element of this method is the correct identification of the mode of oscillation.

The longitudinal mode drives plasma mainly along the magnetic field and produces variations in the plasma density (e.g., Wang 2011). Standing longitudinal oscillations of solar coronal loops were discovered with the Solar Ultraviolet Measurements of Emitted Radiation instrument (SUMER; Wang et al. 2003b) on the *Solar and Heliospheric Observatory* satellite as the periodic Doppler shift of the emission lines Fe xix and Fe xxI, with a formation temperature greater than 6 MK (Wang et al. 2003a; Wang & Solanki 2004). Typical periods are in the range of 8–20 minutes. The oscillations are strongly damped, with the damping timescales equivalent to about one period. Damped oscillations with a period of 69 s and a decay time of 500 s were found in the variations of the H α blue wing emission in a compact C9.6 flare, and interpreted in terms of the second standing harmonics of the longitudinal mode (McAteer et al. 2005). Oscillations in the Doppler velocity of emission lines of S xv and Ca xix, with a formation temperature of 12–14 MK, were observed with *Yohkoh*'s satellite Bragg Crystal Spectrometer (Mariska 2005, 2006) while *Hinode*'s Extreme Ultraviolet (EUV) Imaging Spectrometer allowed observations to be extended to cooler (\sim 1 MK) coronal lines (Mariska et al. 2008; Srivastava & Dwivedi 2010). Longitudinal modes have also been detected as quasi-periodic pulsations (QPPs) in the radio emission generated in solar flares (see, e.g., Nakariakov & Melnikov 2009, for a recent review). Recently, longitudinal oscillations were detected in the microwave 17 GHz emission of a solar flare and simultaneously in the EUV emission intensity measured in the 335 Å channel of the *Solar Dynamics Observatory* Atmospheric Imaging Assembly (Kim et al. 2012). Damped oscillations with a period of 74–88 s were found in the intensity variations of coronal and chromospheric (Ly α) channels of the Large Yield Radiometer experiment (Van Doorsselaere et al. 2011). An example of the simultaneous presence of a 1 minute QPP solar flare in white light emission associated with the chromosphere, and in the microwave and hard X-ray emission from the corona, can be found

⁸ Postdoctoral Fellow of the FWO-Vlaanderen.

⁹ NASA Postdoctoral Program Fellow.

in, e.g., Huang & Ji (2005) and Guangli & Haisheng (2007). The association of optical stellar flares with a bombardment of the lower atmosphere by non-thermal electrons was demonstrated by, (e.g., Osten et al. 2005). The appearance of typical coronal oscillations in white-light emission associated with a flare can hence be connected with the modulation of the precipitation rate of non-thermal electrons. However, details of this process are still poorly understood, as the radiative-hydrodynamic models of dMe flares using a solar-type non-thermal electron beam heating function (Allred et al. 2006) do not produce the $T \approx 9500$ K blackbody spectrum of white-light emission (Mochnacki & Zirin 1980; Hawley & Fisher 1992).

Longitudinal oscillations of coronal loops are associated with standing slow magnetoacoustic oscillations, rapidly damped because of high thermal conduction (Ofman & Wang 2002). Numerical studies (e.g., Nakariakov et al. 2004; Taroyan et al. 2005) demonstrated that this mode can be readily excited by an impulsive energy deposition. The phase speed of the longitudinal waves is the tube speed $C_T = C_s C_A / \sqrt{C_s^2 + C_A^2}$, where C_s and C_A are the sound and Alfvén speeds, respectively (see, e.g., Roberts 2006; Wang 2011). The tube speed is subsonic and sub-Alfvénic. In a low-beta plasma, typical in coronal conditions, the tube speed is just slightly lower than the sound speed. The period of the longitudinal mode is determined by the ratio of the wavelength (i.e., double the length of the loop for the global mode) to the phase speed. Development of this theory for the long-period QPP progressing along the neutral line in a two-ribbon flare has shown that this estimation is robust (Nakariakov & Zimovets 2011; Gruszecki & Nakariakov 2011).

The first detection of a QPP in flares on stars other than the Sun was reported by Rodono (1974) on a flare star in the Hyades using high-speed photoelectric visible photometry. More recent observations include the long-period oscillation (220 s) during the peak of a flare on the active RS Canum Venaticorum binary (RS CVn) II Pegasi (Mathioudakis et al. 2003) and higher frequency oscillations (2–90 s) during the decay phase of flares on the dwarf M stars EQ Pegasi and YZ Canis Minoris (Mathioudakis et al. 2006; Contadakis et al. 2012). Qian et al. (2012) reported a QPP with a mean period of 3 minutes in an *R*-band flare on the red dwarf eclipsing binary CU Cancri. AD Leonis is one of the stars that has been studied extensively in radio wavelengths where high frequency QPPs (0.5–5 s) have been widely observed, often with a varying periodicity (Stepanov et al. 2001; Zaitsev et al. 2004). In soft X-rays, Mitra-Kraev et al. (2005) detected a 750 s oscillation with an exponential damping time of 2000 s during the peak of a flare on AT Microscopium while an oscillation with similar characteristics was detected in the less active binary system ξ Bootis (G8 V+K4 V; Pandey & Srivastava 2009). The interpretations of the stellar flare oscillations reported so far have been primarily based on solar analogs. In particular, the long-period oscillations (longer than several minutes), similar to SUMER oscillations, detected in these stars can be associated with the standing longitudinal mode (Wang 2011).

In this paper, we present white-light observations of rapidly-decaying long QPPs in a powerful “megaflare” on the dM4.5e flare star YZ CMi and discuss possible interpretations.

2. OBSERVATIONS AND ANALYSIS

We analyze a white-light flare on the dM4.5e flare star YZ CMi. The flare began at 04:14:54 UT on 2009 January 16 and had a duration of over 7 hr (Kowalski et al. 2010). At flare peak, the

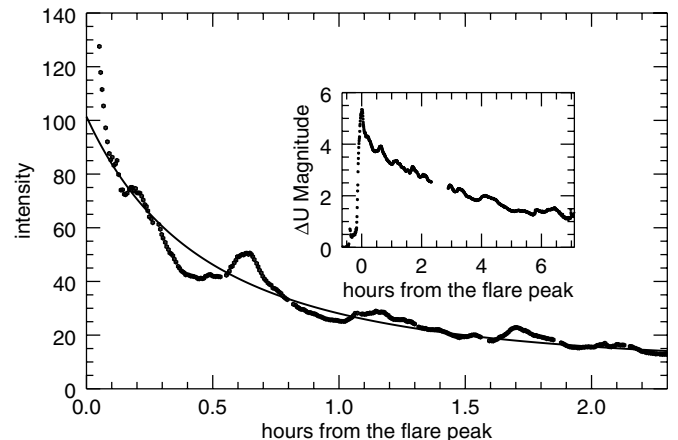


Figure 1. The *U*-band light curve of the YZ CMi megaflare observed on 2009 January 16 (inset). An expanded version of the light curve (black dots) during the decay phase appears in the main figure. The solid line shows the least-squares approximation of the long-term component of the flare profile.

U-band emission was almost 6 mag brighter than the quiescent state. As this was one of the longest and most-energetic flares ever observed in white-light on an isolated low-mass star, it was labeled as a “megaflare.” The observations were acquired with the New Mexico State University 1 m Telescope at the Apache Point Observatory, New Mexico, USA. The star was observed for nearly 8 hr with an exposure time of 10 s; allowing for camera readout, the effective photometric cadence ranged between 20 and 27 s. Differential photometry was performed with HD 62525 as a comparison star.

The light curve, shown in the inset in Figure 1, is typical of that of a white-light flare. It has an impulsive rise to peak before it gradually decays. Such a temporal pattern is typical for stellar flares (see, e.g., Moffett 1974), and in the context of gamma-ray bursts is usually referred to as a “FRED”—Fast Rise, Exponential Decay—pattern (e.g., Fenimore et al. 1996). An inspection of the lightcurve reveals long-period QPPs during the decay phase, which are the subject of our investigation.¹⁰ The relative amplitude of the oscillatory perturbations seen in the decaying trend is about 15%. There is a gap in the data, due to instrument calibration, but this does not affect the time interval of interest.

2.1. Slowly-varying Trends

To extract the oscillatory component from the lightcurve, we split the signal into two components. The first one is the long-term decaying component with a slowly-varying trend. The second one contains the short-term oscillatory variations. To extract the long-term component, we fit the decay phase of the lightcurve with an empirical power-law of the type:

$$I(t) = A(t + 1)^{-d} + I_0, \quad (1)$$

where $I(t)$ is the intensity, t is the time in hours from the flare peak, A is the increase in the intensity at $t = 0$, d is the decay coefficient, and I_0 is the intensity of the background emission. The fitting was done with the COMFIT procedure from the standard Interactive Data Language library (Exelis Visual Information Solutions, Boulder, Colorado). The best-fit result corresponds to the parameters $A = 94.52$, $d = 2.15$, and

¹⁰ Short-period and medium-period QPPs in another flare on this star have been reported by Contadakis et al. (2012).

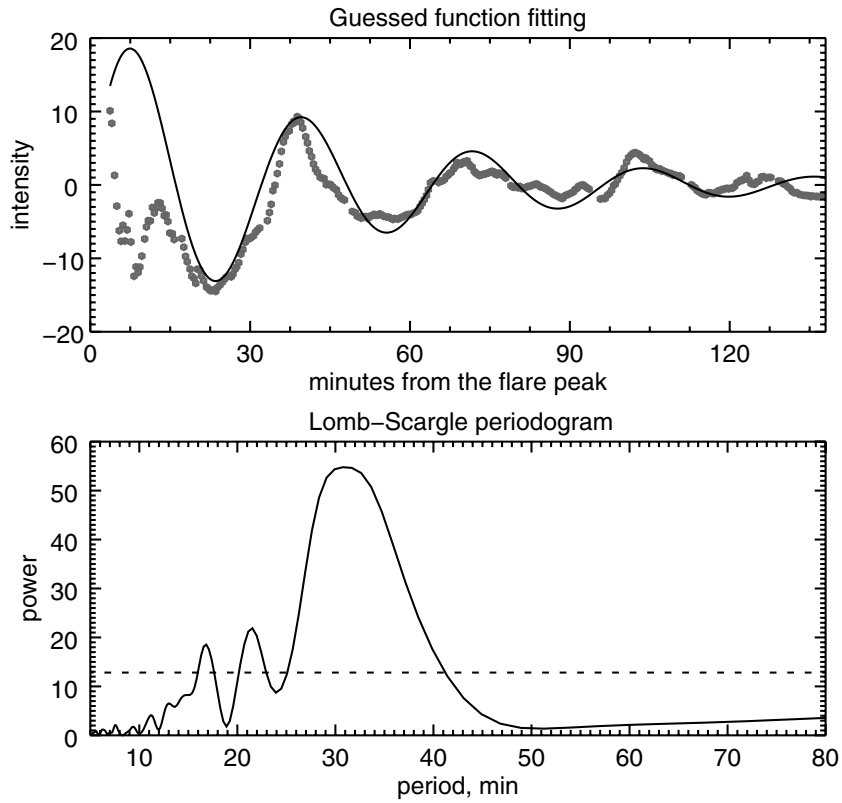


Figure 2. Upper panel: the short-term intensity variations (gray dots) extracted from the U -band light curve. The solid line shows the best-fitting exponentially decaying sinusoidal oscillation, with a period of 32 minutes and a damping time of 46 minutes. Lower panel: the Lomb–Scargle periodogram of the de-trended signal. The horizontal dashed line shows the confidence level of 99.9%.

$I_0 = 6.88$. Subtracting the best-fit power-law function from the original signal, we extract the short-term variation (Figure 2). A similar procedure was used in the extraction of the rapidly-decaying oscillatory signal in the decaying phase of a solar flare (Kim et al. 2012).

2.2. Oscillatory Component

The short term component (upper panel in Figure 2) shows a high-amplitude decaying oscillation. About four cycles of the oscillations are seen. To estimate the oscillation period, we constructed a Lomb–Scargle periodogram (Lomb 1976; Scargle 1982) of the de-trended signal. This method is suitable for unevenly spaced data and is widely used for the detection of periodic signals. The periodogram (lower panel of Figure 2) has a major significant peak at 0.54 mHz that corresponds to a period of about 31 minutes.

As the oscillation is rapidly decaying, the application of spectral methods to study it becomes more complex. A more reliable approach is the approximation of the data by a guessed function. The variations are approximated by the exponentially decaying harmonic function,

$$I(t) = A \cos\left(\frac{2\pi}{P}t + \phi_0\right) \exp\left(-\delta \frac{t}{P}\right), \quad (2)$$

where t is the time from the flare peak, A is the amplitude of the initial perturbation, P is the oscillation period, ϕ_0 is the phase at $t = 0$, and δ is the damping constant. We fit this function to the short-term component to estimate the oscillation parameters. We estimated that the oscillation period is 32 minutes and the damping constant is 0.7, which corresponds to a damping time, $(\delta/P)^{-1}$, of about 46 minutes. Note that the estimated period

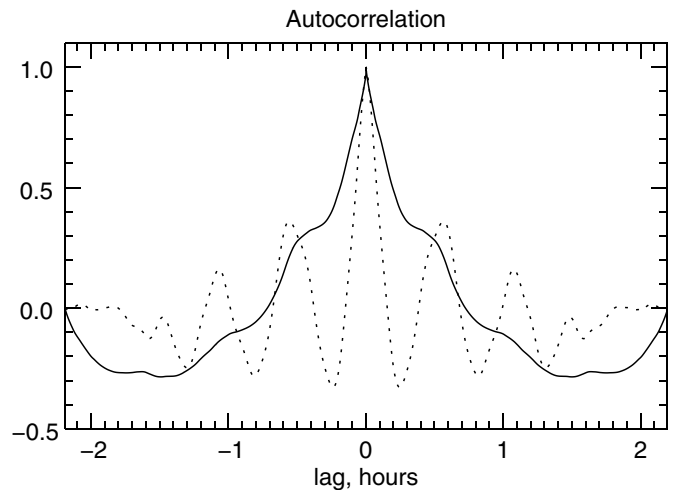


Figure 3. Autocorrelation functions of the decay phase of the light curve of the megaflare. The solid line corresponds to the full signal and the dotted line corresponds to the detrended curve.

is very close to the value obtained with the Lomb–Scargle periodogram. The model curve with these parameters plotted over the short-term component of the light curve is presented in Figure 2. One can see that this model fits the observations well. Some discrepancy between the best-fitted curve and the data can be attributed to the presence of a significant second harmonic with a period of 16 minutes.

To confirm the above findings, we constructed autocorrelation functions of the total signal and of the de-trended signal (Figure 3). This approach suppresses random variations while

emphasizing the periodic pattern in the signal and is often applied in the analysis of flaring QPPs (e.g., Kupriyanova et al. 2010). The autocorrelation function of the detrended signal shows a very clear harmonic pattern with a 32 minute period, which corresponds to the result obtained by the approximation with a guessed function.

3. DISCUSSION

Our analysis shows that the 32 minute QPP detected during the decay phase of this stellar megaflare has a pattern that is typical of the rapidly-decaying long-period oscillations observed in solar flares. Indeed, the oscillation in Figure 2 looks very similar to those shown, e.g., in Figure 4 of Kim et al. (2012), Figure 2 in Mariska (2005), Figure 8 in Wang (2011), Figure 4 in Van Doorsselaere et al. (2011), and Figure 2 in the theoretical paper of Mendoza-Briceño et al. (2004). All of these oscillations have been interpreted as standing longitudinal (slow magnetoacoustic) modes. However, we cannot directly apply previous modeling approaches to the observed QPP. In contrast with the solar observations mentioned earlier, the QPPs presented here are associated with the white-light emission of the cooler photospheric/chromospheric plasma. In our interpretation, we will use the parameters of the YZ CMi corona derived by Raassen et al. (2007): the coronal loops are about 100 Mm, the magnetic field strength in the loops is about 50–100 G, and the electron density is about $3 \times 10^{10} \text{ cm}^{-3}$. These parameters are similar to those in the solar flaring coronal active regions.

The white-light emission most likely originates from the lower, cool layers of the stellar atmosphere (e.g., Haisch et al. 1991; Benz 2008). Light curves of the hard X-ray and white-light emission generated in solar flares are usually similar (see, e.g., Hudson et al. 1992; Metcalf et al. 2003). Moreover, there is evidence of the simultaneous presence of QPPs in the white-light, microwave, and hard X-ray emission of a solar flare (Huang & Ji 2005) and in optical off-band H α and hard X-ray emission (Wang et al. 2000). High correlation of the short-period variability in optical, radio, and hard X-ray emission in a solar flare was also pointed out by Guangli & Haisheng (2007). Thus, it is reasonable to assume that the white-light emission and its variation, including QPPs, are produced by the non-thermal electrons accelerated in the flare.

There are two groups of mechanisms that could provide the observed modulation depth and periodicity:

1. The first group of QPP generation is connected with a periodically modulated flux of precipitating non-thermal electrons. The electrons, interacting with the plasma of the denser layers of the stellar atmosphere, periodically heat it and hence cause the periodic variation of the white-light emission. Below, we list three relevant possibilities.
 - (a) It is a periodic regime of spontaneous magnetic reconnection: there is neither, to the best of our knowledge, a well-developed theory nor unequivocal results of numerical experiments related to this interpretation. However, some numerical experiments show quasi-periodic variations of the reconnection rate (e.g., Kliem et al. 2000; Bárta et al. 2008; Murray et al. 2009). Also, it is not clear whether spontaneous reconnection can provide the decaying harmonic variation of the non-thermal electron production rate. As the reconnection usually occurs during the flare impulsive phase, while the QPPs we study here are seen during the decay phase, we rule out this interpretation.
 - (b) Periodically induced magnetic reconnection and the associated periodically-varying rate of precipitating energetic electrons: this scenario can be associated with different kinds of MHD wave modes. The mechanism for the periodic induction of reconnection by slow magnetoacoustic waves was developed by Chen & Priest (2006), and for fast waves by Nakariakov et al. (2006). Both mechanisms are based on the creation of localized regions of anomalous resistivity in the flare epicenter. The detected period of the oscillation, 32 minutes, allows us to estimate the parameters of the oscillating loop. Assuming a proton concentration of $3 \times 10^{10} \text{ cm}^{-3}$ (Raassen et al. 2007) and a magnetic field strength of 30 G, we obtain an Alfvén speed of 377 km s^{-1} . The value of the magnetic field is lower than in the estimate as we account for the decrease in its strength with height. For the global kink mode, with a speed of 530 km s^{-1} , that is about 40% higher than the Alfvén speed (e.g., Stepanov et al. 2012). The length of the loop should be about 500 Mm (a major radius of about 160 Mm). This value is much larger than the one reported in Raassen et al. (2007). However, it is known that in the solar corona even longer loops can exist, e.g., 500–600 Mm, as detected by Foullon et al. (2010). If we consider the longitudinal (slow magnetoacoustic) mode, for the same value of the Alfvén speed and a sound speed of 300 km s^{-1} , the tube speed is 230 km s^{-1} , resulting in a loop length of about 200 Mm. This value is close to the estimate in Raassen et al. (2007), and is also consistent with the loop length estimated for a flare on a similar M-type dwarf, AT Mic, by Mitra-Kraev et al. (2005). Moreover, analysis of the radio emission generated by a flare on another M-type dwarf, EV Lac, showed that the size of a flaring loop can be larger than or comparable to the stellar radius (Osten et al. 2005), and hence comparable with the value obtained by the above estimate. Thus, both global kink and longitudinal modes can be responsible for the observed periodicity. However, as the time signature of the discussed oscillatory pattern is more consistent with the behavior observed in solar flares in association with longitudinal modes rather than with kink modes, we are inclined to propose that the observed rapidly-decaying oscillation observed here could also be caused by the longitudinal mode.
 - (c) Periodic modulation of non-thermal particle dynamics: periodic variations of the magnetic trapping conditions can be performed by a sausage oscillation in a loop of a non-uniform cross-section (e.g., Zaitsev & Stepanov 2008). These could lead to the periodic precipitation of non-thermal electrons on the dense regions of the stellar atmosphere. However, as the modulating oscillation is essentially of a magnetic nature, the periods should be rather short, seconds or tens of seconds. We therefore tend to rule out this interpretation.
2. The observed periodic variation of the white-light emission during the megaflare could be produced by the periodic occultation of the flare site by an oscillating prominence or filament along the line-of-sight. The oscillation of the prominence could be excited by the flare itself, and could be of sufficiently long period (see, e.g., Hershaw et al. 2011, for a solar example). However, this scenario is not consistent with the observations of this flare in the literature. A passive,

periodic occultation would not produce a simultaneous increase in the white-light and an increase in the amount of hydrogen b-f absorption (Kowalski et al. 2011).

4. CONCLUDING REMARKS

The observed white-light emission originates from the lower layers of a star's atmosphere, the chromosphere or photosphere. The emission is produced by precipitating non-thermal electrons accelerated in the corona where the energy release site lies (e.g., Haisch et al. 1991; Hudson et al. 1992). The oscillatory variation of the emission is hence attributed to the variation in the flux of the precipitating electrons. The flux may be modulated by the non-thermal electron production rate in the reconnection site. The periodic modulation of the reconnection rate or its periodic triggering can be produced by the MHD oscillation of a nearby coronal plasma loop or arcade. The mechanisms for this process have been developed in Chen & Priest (2006) and Nakariakov et al. (2006) for slow and fast waves, respectively. The period and time signature of the observed oscillation in the white-light emission reflect the period and time signature of the MHD oscillation in the loop. Such a quasi-monochromatic oscillation can be readily excited by an initial impulsive energy release in the flare (e.g., Nakariakov et al. 2004; Gruszecki & Nakariakov 2011). The finding of the simultaneous presence of a solar flare's QPP in white-light emission associated with the chromosphere, and in the microwave and hard X-ray emission from the corona (Wang et al. 2000; Huang & Ji 2005; Guangli & Haisheng 2007), supports our conclusion on the coronal origin of the observed QPP in white-light emission. The similarity in the oscillatory pattern detected in the YZ CMi megaflare and the longitudinal oscillations in solar flares suggests that the physical mechanisms responsible for them, i.e., the standing slow magnetoacoustic mode, may be similar to other mechanisms operating over a wide range (10^3) of flare energetics. Other mechanisms, namely, a standing kink oscillation and occultation by an oscillating prominence, cannot be ruled out.

The work is supported by the FP7 Marie Curie PIRSES-GA-2011-295272 *RadioSun* project, the European Research Council under the *SeismoSun* Research Project No. 321141 (VMN), the Russian Ministry of Education and Science project No. 8524, State Contracts 16.518.11.7065 and 02.740.11.0576, the Russian Foundation of Basic Research under grants 12-02-33110-mol-a-ved, 12-02-31746-mol-a, 13-02-00044-a and 13-02-90472-ukr-f-a, and the Kyung Hee University International Scholarship (V.M.N.). T.V.D. has received funding from an Odysseus grant of the FWO-Vlaanderen and from the Framework Programme 7 under grant agreement 276808. M.M. is grateful to the Leverhulme Trust for grant F/00203/X.

REFERENCES

- Allred, J. C., Hawley, S. L., Abbott, W. P., & Carlsson, M. 2006, *ApJ*, **644**, 484
 Bárta, M., Karlický, M., & Žemlička, R. 2008, *SoPh*, **253**, 173
 Benz, A. O. 2008, *LRSP*, **5**, 1
 Chen, P. F., & Priest, E. R. 2006, *SoPh*, **238**, 313
 Contadakis, M. E., Avgoloupis, S. J., & Seiradakis, J. H. 2012, *AN*, **333**, 583
 De Moortel, I., & Nakariakov, V. M. 2012, *RSPTA*, **370**, 3193
 Fenimore, E. E., Madras, C. D., & Nayakshin, S. 1996, *ApJ*, **473**, 998
 Foullon, C., Fletcher, L., Hannah, I. G., et al. 2010, *ApJ*, **719**, 151
 Gruszecki, M., & Nakariakov, V. M. 2011, *A&A*, **536**, A68
 Guangli, H., & Haisheng, J. 2007, *Ap&SS*, **312**, 127
 Haisch, B., Strong, K. T., & Rodono, M. 1991, *ARA&A*, **29**, 275
 Hawley, S. L., & Fisher, G. H. 1992, *ApJS*, **78**, 565
 Hershaw, J., Foullon, C., Nakariakov, V. M., & Verwichte, E. 2011, *A&A*, **531**, A53
 Huang, G., & Ji, H. 2005, *SoPh*, **229**, 227
 Hudson, H. S., Acton, L. W., Hirayama, T., & Uchida, Y. 1992, *PASJ*, **44**, L77
 Kim, S., Nakariakov, V. M., & Shibasaki, K. 2012, *ApJL*, **756**, L36
 Kliem, B., Karlický, M., & Benz, A. O. 2000, *A&A*, **360**, 715
 Kowalski, A. F., Hawley, S. L., Holtzman, J. A., Wisniewski, J. P., & Hilton, E. J. 2010, *ApJL*, **714**, L98
 Kowalski, A. F., Hawley, S. L., Holtzman, J. A., Wisniewski, J. P., & Hilton, E. J. 2011, in IAU Symp. 273, The Physics of Sun and Star Spots, ed. D. P. Choudhary & K. G. Strassmeier (Cambridge: Cambridge Univ. Press), **261**
 Kupriyanova, E. G., Melnikov, V. F., Nakariakov, V. M., & Shibasaki, K. 2010, *SoPh*, **267**, 329
 Lomb, N. R. 1976, *Ap&SS*, **39**, L447
 Mariska, J. T. 2005, *ApJL*, **620**, L67
 Mariska, J. T. 2006, *ApJ*, **639**, 484
 Mariska, J. T., Warren, H. P., Williams, D. R., & Watanabe, T. 2008, *ApJL*, **681**, L41
 Mathioudakis, M., Bloomfield, D. S., Jess, D. B., Dhillon, V. S., & Marsh, T. R. 2006, *A&A*, **456**, 323
 Mathioudakis, M., Seiradakis, J. H., Williams, D. R., et al. 2003, *A&A*, **403**, 1101
 McAteer, R. T. J., Gallagher, P. T., Brown, D. S., et al. 2005, *ApJ*, **620**, 1101
 Mendoza-Briceño, C. A., Erdélyi, R., & Sigalotti, L. D. G. 2004, *ApJ*, **605**, 493
 Metcalf, T. R., Alexander, D., Hudson, H. S., & Longcope, D. W. 2003, *ApJ*, **595**, 483
 Mitra-Kraev, U., Harra, L. K., Williams, D. R., & Kraev, E. 2005, *A&A*, **436**, 1041
 Mochnacki, S. W., & Zirin, H. 1980, *ApJL*, **239**, L27
 Moffett, T. J. 1974, *ApJS*, **29**, 1
 Murray, M. J., van Driel-Gesztelyi, L., & Baker, D. 2009, *A&A*, **494**, 329
 Nakariakov, V. M., Foullon, C., Verwichte, E., & Young, N. P. 2006, *A&A*, **452**, 343
 Nakariakov, V. M., & Melnikov, V. F. 2009, *SSRv*, **149**, 119
 Nakariakov, V. M., Tsiklauri, D., Kelly, A., Arber, T. D., & Aschwanden, M. J. 2004, *A&A*, **414**, L25
 Nakariakov, V. M., & Zimovets, I. V. 2011, *ApJL*, **730**, L27
 Ofman, L., & Wang, T. 2002, *ApJL*, **580**, L85
 Pandey, J. C., & Srivastava, A. K. 2009, *ApJL*, **697**, L153
 Osten, R. A., Hawley, S. L., Allred, J. C., Johns-Krull, C. M., & Roark, C. 2005, *ApJ*, **621**, 398
 Qian, S.-B., Zhang, J., Zhu, L.-Y., et al. 2012, *MNRAS*, **423**, 3646
 Raassen, A. J. J., Mitra-Kraev, U., & Güdel, M. 2007, *MNRAS*, **379**, 1075
 Roberts, B. 2006, *RSPTA*, **364**, 447
 Roberts, B., Edwin, P. M., & Benz, A. O. 1984, *ApJ*, **279**, 857
 Rodono, M. 1974, *A&A*, **32**, 337
 Scargle, J. D. 1982, *ApJ*, **263**, 835
 Srivastava, A. K., & Dwivedi, D. N. 2010, *NewA*, **15**, 8
 Stepanov, A. V., Kliem, B., Zaitsev, V. V., et al. 2001, *A&A*, **374**, 1072
 Stepanov, A. V., Zaitsev, V. V., & Nakariakov, V. M. 2012, *Coronal Seismology* (1st ed.; Weinheim: Wiley-VCH)
 Taroyan, Y., Erdélyi, R., Doyle, J. G., & Bradshaw, S. J. 2005, *A&A*, **438**, 713
 Van Doorsselaere, T., De Groof, A., Zender, J., Berghmans, D., & Goossens, M. 2011, *ApJ*, **740**, 90
 Wang, H., Qiu, J., Denker, C., et al. 2000, *ApJ*, **542**, 1080
 Wang, T. 2011, *SSRv*, **158**, 397
 Wang, T. J., & Solanki, S. K. 2004, *A&A*, **421**, L33
 Wang, T. J., Solanki, S. K., Curdt, W., et al. 2003, *A&A*, **406**, 1105
 Wang, T. J., Solanki, S. K., Innes, D. E., Curdt, W., & Marsch, E. 2003, *A&A*, **402**, L17
 Zaitsev, V. V., Kislyakov, A. G., Stepanov, A. V., Kliem, B., & Furst, E. 2004, *AstL*, **30**, 319
 Zaitsev, V. V., & Stepanov, A. V. 1975, *IGAFS*, **37**, 3
 Zaitsev, V. V., & Stepanov, A. V. 2008, *PhyU*, **51**, 1123